The 9th European Congress on Computational Methods in Applied Sciences and Engineering
ECCOMAS Congress 2024
3–7 June 2024, Lisboa, Portugal

HIERARCHIC LARGE ROTATION SHELL MODEL WITH WARPING: ISOGEOMETRIC FORMULATION AND MODELING OF ALTERNATING STIFF/SOFT LAMINATES

DOMENICO MAGISANO[1], ANTONELLA CORRADO[1], LEONARDO LEONETTI[1], JOSEF KIENDL[2] AND GIOVANNI GARCEA[1]

[1] Department of Computer Science, Modeling, Electronics and Systems Engineering,
University of Calabria, 87030 Rende (Cosenza), Italy
e-mail: domenico.magisano@unical.it
[2] Institute of Engineering Mechanics and Structural Analysis,
Bundeswehr University Munich, Werner-Heisenberg-Weg 39, 85577 Neubiberg, Germany
e-mail: josef.kiendl@unibw.de

Key words: Composite shells, warping, large deformation, buckling, isogeometric analysis

Summary. This paper presents a hierarchic large rotation Kirchhoff-Love shell model with warping. Two unknowns are introduced for each through-the-thickness function warping, representing its amplitudes in two directions tangent to the shell surface. NURBS are used to approximate reference surface displacement and warping amplitudes in the weak form. The transverse shear strains depend only on the warping parameters linearly and are free from locking. A patch-wise reduced integration avoids membrane locking and improves efficiency. Focus is given to composites made up of multiple stiff layers coupled with soft interlayers. The alternating layup with high stiffness ratios induces a significant sectional warping with transverse shear strains concentrated in the soft layers. Two warping models are investigated: WI) all stiff layers maintain the same director orthogonal to the deformed surface with independent transverse shear deformations of the soft layers; WZ) a single zigzag function linking these deformations. The numerical tests confirm the great accuracy of the hierarchic shell model in reproducing the solid solution with a small number of discrete parameters, provided that the correct warping model is chosen. WI is reliable for all alternating layups. WZ reduces the unknowns to five per surface point, regardless of the number of layers, and is accurate for uniform soft layers.

1 INTRODUCTION

Laminated composites are obtained by a piling of layers of different materials, or of plies of the same material but with different orientation, as in fiber-reinforced composites. The non-uniform distribution of the material properties over the thickness direction accentuates a certain deformation phenomenology: transverse shear strains become important and the planarity of the deformed section is often lost even for rather slender structures. Each layer may exhibit a different angle of rotation and the final configuration of the deformed cross-section assumes a zigzag shape, that is a piece-wise linear configuration. Although the application of these materials is now widespread, the development of accurate and affordable analysis and design methods is still an open topic in the scientific community, in particular because the layup configuration influences significantly the modeling rules. Concerning plate/shell models, two main approaches

are usually followed: the equivalent single-layer theories (ESL) and the layer-wise theories (LW).

Multi-layered composite shells made of a number of stiff plies shear-coupled by soft interlayers are a typical case of laminates whose mechanics is dominated by the zigzag effects. Among many others, typical examples are represented by laminated glass and metal-polymer laminates, i.e. glass or metal plies bonded by polymeric interlayers. Although the soft interlayers have in practice no bending stiffness by themselves, they can restrain the shear-sliding of the stiff plies increasing the overall bending capacity of the laminate [1], which varies [2] between the lower bound of free-sliding stiff plies (layered limit) and the upper-bound of perfectly coupled plies (monolithic limit). The alternating layup induces a specific straining/deformation pattern, which distinguishes them from other composites [3, 4]. In fact, the transverse shear strains tend to concentrate in the soft interlayers, with a nearly constant distribution in the thickness, while they are negligible in the stiff plies. Moreover, although the interlayers are soft, they constrain the relative distance between the surfaces to which they adhere. The consequence is that the stiff layers are all subjected to almost identical rotations with respect with their normals in the initial configuration, while the soft layers undergo independent transverse shear strains. Different plate/shell models have been proposed for alternating layups. A reference paper in the field is [3] where, for the first time, a shell model imposing equal rotation of the stiff layers and independent shear deformations of the soft interlayers was proposed. This is a Mindlin-Reissner model enriched by independent in-plane displacements of the soft layers. The same work implements a locking-free shell finite element with the geometrically nonlinear model recovered by the co-rotational approach [5]. The kinematics with independent shear deformations of the soft layers [3] results useful also for including thermal and viscous effects [6] and for modeling more general boundary conditions. Most often, the stiff layers tend to exhibit negligible transverse shear strains. Although limited to small-displacement analyses, the Kirchhoff-Love assumption of neglecting the transverse shear strains in the stiff layers was exploited in [4], with the aim of further reducing the model variables. The C^1 continuity requirement is met with special finite elements. In [7] a hierarchic implementation of the Refined Zig Zag theory (ZZT) [8] is proposed, adopting finite elements based on the geometrically exact shell theory of Simo [9], in order to economically describe the behavior of composite laminates undergoing large deformations but small strains by adding only two additional DOFs. A linear finite element approximation of geometry and kinematics is considered in this work.

In [10], a nonlinear KL model is extended hierarchically with linearized transverse shear components. Two formulations are proposed, using hierarchic rotations or hierarchic displacement to include the transverse shear effects. The basic assumption, confirmed by numerical investigation, is that the transverse shear strains remain small in most simulations involving large deflections.

Inspired by this work, this paper proposes a large deformation/small strain Kirchhoff-Love shell model hierarchically enhanced with warping. The warping displacement is additional with respect to the arbitrarily large displacement of the shell reference surface. Hence, it is purely deformational, i.e. not affected by rigid body motions, and small allowing an additive split of the strain into the nonlinear part of the basic Kirchhoff-Love model and a linear part of the additional warping deformation. The resulting model is geometrically exact, in the sense that the overall strain measure is not influenced by arbitrarily large rigid motions. Warping is described as combination of a number of through-the-thickness shape functions, generically selected by the user. Two unknowns are introduced for each warping shape, representing its amplitudes in two directions tangent to the shell surface. The plane stress condition is exploited as usual. In the

framework of the isogeometric analysis, NURBS basis functions are used to approximate reference surface displacement and warping amplitudes, in order to meet the continuity requirement of the weak form. The transverse shear strains depend only on the warping amplitudes. They are linear with the corresponding DOFs and naturally free from locking. Membrane locking is avoided by a proper choice of the basis functions degree and the adoption of an efficient patch-wise reduced integration scheme for the strain energy associated to the in-plane strain components, the only integration to be repeated in the nonlinear analysis. Particular focus is given to the modeling of composite plates and shells with alternating stiff/soft layups, for which two warping models are investigated. The first one assumes that all stiff layers maintain the same director orthogonal to the deformed surface with independent transverse shear deformations of the soft layers. This can be considered as an exact geometry, Total-Lagrangian, rotation-free, higher order version of the proposal in [3], that exploits the negligible transverse shear deformations of the stiff layers to reduce the number of variables per surface point. A second model uses a single zigzag function linking the transverse shear deformations of the soft layers to further reduce the variables to five per surface point, regardless of the number of layers. A set of numerical tests is reported to assess the validity of the hierarchic formulation and the coarse-mesh accuracy of the discretization. In addition, a critical evaluation of the reliability of the two warping models compared to the solid solution is carried out, showing in which cases one model is preferable to the other.

The article is organized as follows. After a brief introduction to the Kirchhoff-Love shell model, Section 2 formulates the Kirchhoff-Love model hierarchically enhanced with generic warping functions in a large deformation/small strain context. Warping models for laminates with alternating stiff/soft layups are presented in Section 3. Details concerning the isogeometric discretization and the nonlinear analysis are reported in Section 4. Section 5 contains a significant set of numerical tests. Conclusions are drawn in Section 6.

2 HIERARCHIC KIRCHHOFF-LOVE SHELL MODEL WITH WARPING

2.1 Standard Kirchhoff-Love shell

A set of convective coordinates ξ^α, with $\alpha = 1, 2$ is considered over a suitable reference shell surface (not necessarily being the middle surface of the shell), while in the thickness direction the coordinate $\xi^3 \in [\xi^3_b, \xi^3_t]$ is assumed with ξ^3_b and ξ^3_t identifying the offset of bottom and top surfaces of the body with respect to the reference one. The position of a point in the undeformed configuration is defined by the position vector $\mathbf{X}$

$$\mathbf{X} = \mathbf{R}(\xi^1, \xi^2) + \xi^3 \mathbf{A}_3(\xi^1, \xi^2) \tag{1}$$

where $\mathbf{R}(\xi^1, \xi^2)$ represents the position of the corresponding point on the reference surface and $\mathbf{A}_3$ the initial shell normal taken as

$$\mathbf{A}_3 = \frac{\mathbf{A}_1 \times \mathbf{A}_2}{|\mathbf{A}_1 \times \mathbf{A}_2|}. \tag{2}$$

with vectors

$$\mathbf{A}_\alpha = \frac{\partial \mathbf{R}}{\partial \xi^\alpha} \qquad \text{with} \quad \alpha = 1, 2$$

defining a tangent plane to the shell surface. Covariant base vectors $\mathbf{G}_\alpha$ in the reference configuration can be then evaluated as

$$\begin{aligned} \mathbf{G}_\alpha &= \frac{\partial \mathbf{X}}{\partial \xi^\alpha} = \mathbf{A}_\alpha + \xi^3 \mathbf{A}_{3,\alpha} \qquad \text{with} \quad \alpha = 1,2 \\ \mathbf{G}_3 &= \frac{\partial \mathbf{X}}{\partial \xi^3} = \mathbf{A}_3 \end{aligned} \tag{3}$$

The current deformed configuration is described as

$$\mathbf{x} = \mathbf{r}(\xi^1, \xi^2) + \xi^3 \mathbf{a}_3(\xi^1, \xi^2) \tag{4}$$

where $\mathbf{r} = \mathbf{R} + \mathbf{v}$ is the current position of the reference surface, with $\mathbf{v}$ its displacement. Introducing the reference surface covariant basis vectors in the deformed configuration

$$\mathbf{a}_\alpha = \frac{\partial \mathbf{r}}{\partial \xi_\alpha} = \mathbf{A}_\alpha + \mathbf{v}_{,\alpha} \qquad \text{with} \quad \alpha = 1,2$$

the current normal is defined as

$$\mathbf{a}_3 = \frac{\mathbf{a}_1 \times \mathbf{a}_2}{|\mathbf{a}_1 \times \mathbf{a}_2|}, \tag{5}$$

according to the Kirchhoff-Love shell assumption that the director remains straight and normal to the shell surface during deformation. The covariant basis vectors in the deformed configuration can be computed over the body as

$$\begin{aligned} \mathbf{g}_\alpha &= \frac{\partial \mathbf{x}}{\partial \xi^\alpha} = \mathbf{a}_\alpha + \xi^3 \mathbf{a}_{3,\alpha} \qquad \text{with} \quad \alpha = 1,2 \\ \mathbf{g}_3 &= \frac{\partial \mathbf{x}}{\partial \xi^3} = \mathbf{a}_3(\xi^1, \xi^2) \end{aligned} \tag{6}$$

Denoting the displacement of the body with

$$\mathbf{u} = \mathbf{x} - \mathbf{X} = \mathbf{v}(\xi^1, \xi^2) + \xi^3 (\mathbf{a}_3(\xi^1, \xi^2) - \mathbf{A}_3(\xi^1, \xi^2)) \tag{7}$$

the Green-Lagrange strain tensor can be written as

$$\mathbf{E} = \sum_{i,j=1}^{3} \bar{E}_{ij} \mathbf{G}^i \otimes \mathbf{G}^j \quad \text{with} \quad \bar{E}_{ij} = \frac{1}{2} (\mathbf{g}_i \cdot \mathbf{g}_j - \mathbf{G}_i \cdot \mathbf{G}_j) = \frac{1}{2} (\mathbf{u}_{,i} \cdot \mathbf{G}_j + \mathbf{u}_{,j} \cdot \mathbf{G}_i + \mathbf{u}_{,i} \cdot \mathbf{u}_{,j}) \tag{8}$$

where $\bar{E}_{ij}$ are the covariant strain components. The partial derivatives of the displacement vector are

$$\begin{aligned} \mathbf{u}_{,\alpha} &= \mathbf{v}_{,\alpha} + \xi^3 (\mathbf{a}_{3,\alpha} - \mathbf{A}_{3,\alpha}) \qquad \text{with} \quad \alpha = 1,2 \\ \mathbf{u}_{,3} &= \mathbf{a}_3(\xi^1, \xi^2) - \mathbf{A}_3(\xi^1, \xi^2) \end{aligned} \tag{9}$$

The reference surface and body contravariant basis vectors are obtained from the dual basis condition $\mathbf{a}_\alpha \cdot \mathbf{a}^\beta = \mathbf{A}_\alpha \cdot \mathbf{A}^\beta = \delta_\alpha^\beta$ and $\mathbf{g}_\alpha \cdot \mathbf{g}^\beta = \mathbf{G}_\alpha \cdot \mathbf{G}^\beta = \delta_\alpha^\beta$, with $\alpha, \beta = 1,2$. Due to Eq. (2) and (5), the transverse shear strains vanish, that is $\bar{E}_{\alpha 3} = 0, \quad \alpha = 1,2$. The same holds for the thickness strain, i.e. $\bar{E}_{33} = 0$. Assuming its components to vary linearly through the thickness,

it is possible to separate the strain into a constant part due to membrane action and a linear part due to bending. The covariant strain coefficients are:

$$\bar{E}_{\alpha\beta} = \bar{e}_{\alpha\beta} + \xi^3 \bar{\chi}_{\alpha\beta} = \frac{1}{2}(a_{\alpha\beta} - A_{\alpha\beta}) + \xi^3 (B_{\alpha\beta} - b_{\alpha\beta}) \quad \text{with} \quad \alpha, \beta = 1, 2 \tag{10}$$

with the metric coefficients $a_{\alpha\beta} = \mathbf{a}_\alpha \cdot \mathbf{a}_\beta$ and $A_{\alpha\beta} = \mathbf{A}_\alpha \cdot \mathbf{A}_\beta$ with $\alpha, \beta = 1, 2$. The curvature tensor coefficients [11] are defined as

$$\begin{aligned} B_{\alpha\beta} &= -\frac{1}{2}(\mathbf{A}_\alpha \cdot \mathbf{A}_{3,j} + \mathbf{A}_\beta \cdot \mathbf{A}_{3,\alpha}) = \mathbf{A}_{\alpha,\beta} \cdot \mathbf{A}_3 \\ b_{\alpha\beta} &= -\frac{1}{2}(\mathbf{a}_\alpha \cdot \mathbf{a}_{3,j} + \mathbf{a}_\beta \cdot \mathbf{a}_{3,\alpha}) = \mathbf{a}_{\alpha,\beta} \cdot \mathbf{a}_3 \end{aligned} \tag{11}$$

The curvature components for the Kirchhoff-Love shell can be then computed as

$$\bar{\chi}_{\alpha\beta} = B_{\alpha\beta} - b_{\alpha\beta} = \mathbf{A}_{\alpha,\beta} \cdot \mathbf{A}_3 - \mathbf{a}_{\alpha,\beta} \cdot \mathbf{a}_3 \quad \text{with} \quad \alpha, \beta = 1, 2$$

The presence of the norm $|\mathbf{a}_1 \times \mathbf{a}_2|$ in the denominator of $\mathbf{a}_3$ leads to a rather complicated expression of the curvature in terms of the displacement field and, then, a computationally expensive evaluation of the discrete operators coming from the strain variations. A simplified formula for the curvature proposed in [12] is here adopted, exploiting the hypothesis of large deformations but small membrane strains. It is based on the following simplification in Eq. (5):

$$|\mathbf{a}_1 \times \mathbf{a}_2| \approx |\mathbf{A}_1 \times \mathbf{A}_2|.$$

Consequently, $b_{\alpha\beta}$ is simplified as

$$b_{\alpha\beta} \approx \mathbf{a}_{\alpha,\beta} \cdot \frac{\mathbf{a}_1 \times \mathbf{a}_2}{|\mathbf{A}_1 \times \mathbf{A}_2|}.$$

and the curvature components reduce to

$$\bar{\chi}_{\alpha\beta} = B_{\alpha\beta} - b_{\alpha\beta} \approx \frac{1}{|\mathbf{A}_1 \times \mathbf{A}_2|}(\mathbf{A}_{\alpha,\beta} \cdot (\mathbf{A}_1 \times \mathbf{A}_2) - \mathbf{a}_{\alpha,\beta} \cdot (\mathbf{a}_1 \times \mathbf{a}_2)) \quad \alpha, \beta = 1, 2 \tag{12}$$

that is a third order dependence on the displacement. The in-plane strain components of the KL model can be written in Voigt's notation as

$$\bar{\boldsymbol{\varepsilon}}_p = \bar{\mathbf{e}} + \xi^3 \bar{\boldsymbol{\chi}} \quad \text{with} \quad \bar{\boldsymbol{\varepsilon}}_p = \begin{bmatrix} \bar{E}_{11} \\ \bar{E}_{22} \\ 2\bar{E}_{12} \end{bmatrix}, \quad \bar{\mathbf{e}} = \begin{bmatrix} \bar{e}_{11} \\ \bar{e}_{22} \\ 2\bar{e}_{12} \end{bmatrix}, \quad \bar{\boldsymbol{\chi}} = \begin{bmatrix} \bar{\chi}_{11} \\ \bar{\chi}_{22} \\ 2\bar{\chi}_{12} \end{bmatrix}. \tag{13}$$

2.2 Hierarchic shell model with warping

Multiple warping deformations, assumed to be small, can be hierarchically added to the KL shell kinematics. Let us consider the case of an overall warping profile expressed as a combination of n shapes $w_k(\xi^3)$. The current configuration is defined as:

$$\mathbf{x} = \mathbf{r}(\xi^1, \xi^2) + \xi^3 \mathbf{a}_3(\xi^1, \xi^2) + \sum_{k=1}^{n} \sum_{\beta=1}^{2} \mu_{\beta k}(\xi^1, \xi^2) w_k(\xi^3) \mathbf{a}_\beta(\xi_1, \xi_2) \tag{14}$$

where $\mu_{\beta k}(\xi^1,\xi^2)$ represents the amplitude of the kth warping shape directed along the surface tangent vectors $\mathbf{a}_\beta$ with $\beta = 1,2$ respectively. The profile is assumed to be approximated by the same shapes (with different amplitudes) along the 2 directions, as typical for example for composites made of isotropic layers, also if the generalization to different shapes could be considered for generic composites [7]. The covariant base vectors are defined as:

$$\begin{aligned}\mathbf{g}_\alpha &= \frac{\partial \mathbf{x}}{\partial \xi^\alpha} = \mathbf{a}_\alpha + \xi^3 \mathbf{a}_{3,\alpha} + \sum_{k=1}^{n}\sum_{\beta=1}^{2}\left(\mu_{\beta k}(\xi^1,\xi^2) w_k(\xi^3)\mathbf{a}_{\beta,\alpha} + \mu_{\beta k,\alpha}\, w_k(\xi^3)\mathbf{a}_\beta\right), \quad \alpha = 1,2 \\ \mathbf{g}_3 &= \frac{\partial \mathbf{x}}{\partial \xi^3} = \mathbf{a}_3(\xi^1,\xi^2) + \sum_{k=1}^{n}\sum_{\beta=1}^{2}\mu_{\beta k} w_{k,3}\,\mathbf{a}_\beta(\xi_1,\xi_2)\end{aligned} \tag{15}$$

Using (14) and (1), the displacement field assumes the expression:

$$\mathbf{u} = \mathbf{x} - \mathbf{X} = \underbrace{\mathbf{v}(\xi^1,\xi^2) + \xi^3(\mathbf{a}_3(\xi^1,\xi^2) - \mathbf{A}_3(\xi^1,\xi^2))}_{\mathbf{u}^{KL}} + \underbrace{\sum_{k=1}^{n}\sum_{\beta=1}^{2}\mu_{\beta k} w_k(\xi^3)\mathbf{a}_\beta(\xi_1,\xi_2)}_{\mathbf{u}^{Z}} \tag{16}$$

where $\mathbf{u}^{KL}$ represents the displacement coming from the KL model and $\mathbf{u}^Z$ is the contribution given by warping. Analogously, the derivatives of the displacements can be expressed as the sum of the KL and warping contributions:

$$\begin{aligned}\mathbf{u}_{,\alpha} &= \mathbf{u}^{KL}_{,\alpha} + \mathbf{u}^{Z}_{,\alpha} \quad \text{with} \quad \mathbf{u}^{Z}_{,\alpha} = \sum_{k=1}^{n}\sum_{\beta=1}^{2}(\mu_{\beta k}\mathbf{a}_{\beta,\alpha} + \mu_{\beta k,\alpha}\,\mathbf{a}_\beta) w_k, \quad \alpha = 1,2 \\ \mathbf{u}_{,3} &= \mathbf{u}^{KL}_{,3} + \mathbf{u}^{Z}_{,3} \quad \text{with} \quad \mathbf{u}^{Z}_{,3} = \sum_{k=1}^{n}\sum_{\beta=1}^{2}\mu_{\beta k}\mathbf{a}_\beta w_{k,3}\end{aligned} \tag{17}$$

The covariant strain components can be linearized with respect to the warping amplitudes, collected in vector $\boldsymbol{\mu}$, as

$$\bar{E}_{ij} = \underbrace{\left[\bar{E}_{ij}\right]_{\boldsymbol{\mu}=\mathbf{0}}}_{\bar{E}^{KL}_{ij}} + \underbrace{\left[\frac{\partial \bar{E}_{ij}}{\partial \boldsymbol{\mu}}\right]_{\boldsymbol{\mu}=\mathbf{0}} \cdot \boldsymbol{\mu}}_{\bar{E}^{Z}_{ij}}, \quad \text{with} \quad i,j = 1,2,3 \tag{18}$$

and, neglecting terms more than linear in ξ^3 and w_α, we obtain the additional warping contribution to the strain.

In compact notation, the in-plane warping strains are

$$\bar{\boldsymbol{\varepsilon}}^z_p = \begin{bmatrix}\bar{E}^z_{11}\\ \bar{E}^z_{22}\\ \bar{E}^z_{12}\end{bmatrix} = \sum_{k=1}^{n}\bar{\boldsymbol{\psi}}_k w_k, \qquad \bar{\boldsymbol{\psi}}_k \approx \sum_{\beta=1}^{2}\begin{bmatrix}\mu_{\beta k}\mathbf{A}_1\cdot\mathbf{A}_{\beta,1} + \mu_{\beta k,1}\,\mathbf{A}_1\cdot\mathbf{A}_\beta \\ \mu_{\beta k}\mathbf{A}_2\cdot\mathbf{A}_{\beta,2} + \mu_{\beta k,2}\,\mathbf{A}_2\cdot\mathbf{A}_\beta \\ \mu_{\beta k}(\mathbf{A}_1\cdot\mathbf{A}_{\beta,2} + \mathbf{A}_2\cdot\mathbf{A}_{\beta,1}) + \mu_{\beta k,2}\,\mathbf{A}_1\cdot\mathbf{A}_\beta + \mu_{\beta k,1}\,\mathbf{A}_2\cdot\mathbf{A}_\beta\end{bmatrix}. \tag{19}$$

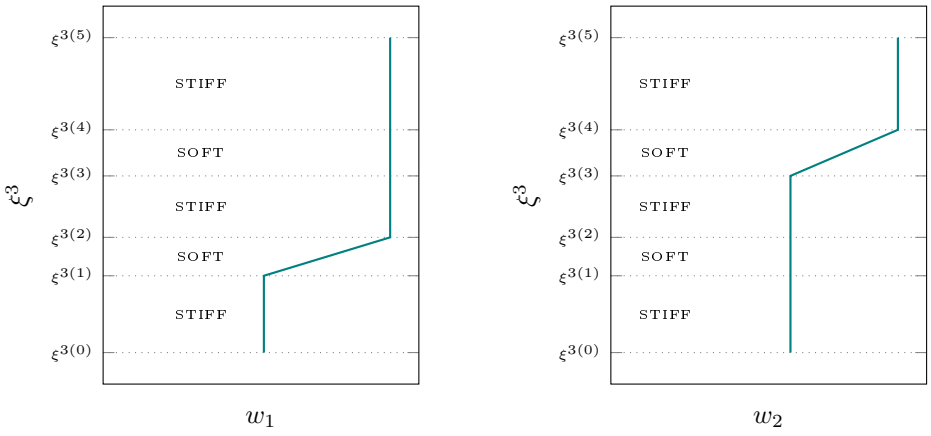

(a) (b)

Figure 1: Warping functions with independent transverse shear deformations of the soft interlayers (WI) for 5 alternating stiff/soft layers.

and the transverse shear ones are

$$\bar{\boldsymbol{\varepsilon}}_t^z = \begin{bmatrix} 2\bar{E}_{13}^z \\ 2\bar{E}_{23}^z \end{bmatrix} = \sum_{k=1}^{n} \bar{\gamma}_k w_{k,3}\,, \quad \bar{\gamma}_k \approx \sum_{\beta=1}^{2} \begin{bmatrix} \mu_{\beta k}\mathbf{A}_1 \cdot \mathbf{A}_\beta \\ \mu_{\beta k}\mathbf{A}_2 \cdot \mathbf{A}_\beta \end{bmatrix}. \tag{20}$$

under the condition of large deformations but small strains ($\mathbf{a}_\alpha \cdot \mathbf{a}_\beta \approx \mathbf{A}_\alpha \cdot \mathbf{A}_\beta$, $\mathbf{a}_\alpha \cdot \mathbf{a}_{\beta,1} \approx \mathbf{A}_\alpha \cdot \mathbf{A}_{\beta,1}$ and $\mathbf{a}_\alpha \cdot \mathbf{a}_{\beta,2} \approx \mathbf{A}_\alpha \cdot \mathbf{A}_{\beta,2}$ with $\alpha, \beta = 1, 2$). The equivalence of strain energy per unit of reference surface in terms of Cartesian strains

$$W = \frac{1}{2}\int_{\xi_b^3}^{\xi_t^3} (\boldsymbol{\varepsilon}_p^T \mathbf{C}_p \boldsymbol{\varepsilon}_p + \boldsymbol{\varepsilon}_t^T \mathbf{C}_t \boldsymbol{\varepsilon}_t) d\xi^3 = \frac{1}{2}(\boldsymbol{\varepsilon}_P^T \mathbf{D}_P \boldsymbol{\varepsilon}_P + \boldsymbol{\varepsilon}_T^T \mathbf{D}_T \boldsymbol{\varepsilon}_T) \tag{21}$$

provides the generalized constitutive matrices.

3 WARPING MODEL

3.1 Warping with independent transverse shear deformations of the soft layers

This warping profile is chosen as proposed for the first time in [3]. In practice, a number of warping profiles equal to the soft interlayers is considered. The same profiles, but with independent amplitudes, can be assumed along both the directions defined by the tangent vectors $\mathbf{A}_1$ and $\mathbf{A}_2$. The total number of variables of the model at each point over the shell surface is $n_t = 3 + 2n_s$: 3 components of the reference surface displacement and 2 amplitudes for the warping profile associated to each of the n_s soft layers. For the case of 5 layers, the 2 warping functions are illustrated in Fig. 1.

3.2 Warping with a single zigzag shape

The refined ZZT provides a single piecewise linear shape of the warping profile over the whole thickness of the laminate, denoted in following as $w(\xi^3)$, avoiding the subscript k previously used

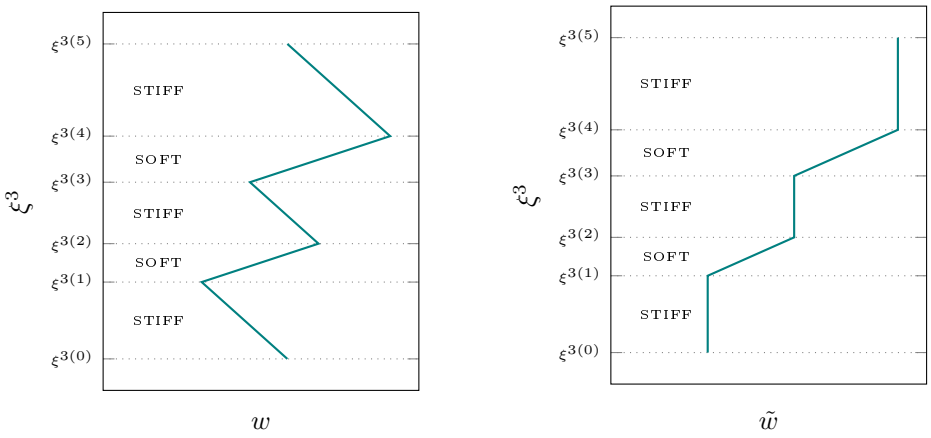

(a) ZZ function (b) Rotated ZZ function

Figure 2: Zigzag warping function (WZ) for 5 alternating stiff/soft layers: the function coming from the refined ZZT on the left and the function rotated in order to minimize the shear deformation of the stiff layers on the right.

in the case of multiple shapes. According to this theory, the zigzag function is defined by the $N+1$ interface values $w^{(j)}$, with $j = 0, 1, ...N$ and N the overall number of layers. The theory sets $w(\xi^3)$ to vanish at the top and bottom surfaces of the laminate, i.e. $w^{(0)} = w^{(N)} = 0$. The internal interface values are computed as

$$w^{(j)} = w^{(j-1)} + h^{(j)}\beta^{(j)} \quad \text{with} \quad j = 1, ..., N-1 \tag{22}$$

where $h^{(j)}$ is the thickness of the jth layer. $\beta^{(j)}$ is the slope of the zigzag function in each layer j, and is obtained as

$$\beta^{(j)} = \frac{\bar{G}}{G^{(j)}} - 1 \quad \text{with} \quad j = 1, ..., N \tag{23}$$

where $G^{(j)}$ is the shear modulus of the jth layer and $\bar{G}$ denotes a weighted average of G over the laminate thickness, i.e.

$$\bar{G} = \left(\frac{1}{h} \sum_{j=1}^{N} \frac{h^{(j)}}{G^{(j)}} \right)^{-1} \tag{24}$$

The complete derivation of these equations can be found in [13]. Let us consider a layup made of 5 alternating stiff/soft layers. As we can observe on the left side of Fig. 2, the constraint of vanishing zigzag function at the top and bottom surfaces produces a profile characterized by non-null slop, and then transverse shear strain, in all layers including the stiff ones.

Starting from the one obtained with the formulas above, the rotated zigzag function $\tilde{w}$ is obtained as

$$\tilde{w}(\xi^3) = w(\xi^3) - \varphi\xi^3 \quad \text{with} \quad \varphi = \frac{\sum_{j=1}^{N} G^{(j)} h^{(j)} \beta^{(j)}}{\sum_{j=1}^{N} G^{(j)} h^{(j)}} \tag{25}$$

where φ represents a weighted average of the zigzag function slop over the laminate thickness, in order to concentrate the transverse shear deformation in the soft layers only. Finally, a rigid

displacement, e.g. the value of $\tilde{w}(\xi^3)$ at the reference shell surface, can be also subtracted to $\tilde{w}$ for an easy imposition of the support boundary condition. The rotated zigzag function is illustrated on the right side of Fig. 2 for a layup with 5 alternating stiff/soft layers. The resulting shell model is accurate also when the zigzag effects become important, although based on just 5 DOFs per reference surface point, i.e. 3 displacements and the 2 amplitudes of $\tilde{w}$ along the two directions identified by the tangent vectors $\mathbf{A}_1$ and $\mathbf{A}_2$, regardless of the number of layers.

4 THE ISOGEOMETRIC SHELL ELEMENT

Following the isoparametric concept, geometry and displacement field of the reference surface and warping amplitudes are approximated, over each element, as follows

$$\mathbf{X}(\xi,\eta) = \mathbf{N}_u(\xi,\eta)\mathbf{X}_e, \quad \mathbf{u}(\xi,\eta) = \mathbf{N}_u(\xi,\eta)\mathbf{d}_e, \quad \boldsymbol{\mu}(\xi,\eta) = \mathbf{N}_\mu(\xi,\eta)\boldsymbol{\mu}_e \tag{26}$$

where $\mathbf{X}_e$, $\mathbf{d}_e$ and $\boldsymbol{\mu}_e$ collect the discrete parameters at the control points of the element associated to geometry, reference surface displacement and warping amplitudes respectively. The matrices $\mathbf{N}_u(\xi,\eta)$ and $\mathbf{N}_\mu(\xi,\eta)$ collect bivariate NURBS functions [14]. Exploiting the isogeometric approximation, the strain components become

$$\boldsymbol{\varepsilon}_P = \boldsymbol{\varepsilon}_P(\mathbf{q}_e) \qquad \boldsymbol{\varepsilon}_T = \boldsymbol{\varepsilon}_T(\mathbf{q}_e) \quad \text{with} \quad \mathbf{q}_e = \begin{bmatrix} \mathbf{d}_e \\ \boldsymbol{\mu}_e \end{bmatrix}. \tag{27}$$

We adopt cubic NURBS basis functions with C^2 continuity and the patch-wise reduced integration named S_0^3 ([15]) to avoid membrane locking. The nonlinear load-displacement curves are traced using the Riks arc-length method improved with MIP (Mixed Integration Point) Newton iterative solver [16, 17].

5 NUMERICAL TESTS

The layups illustrated in Fig. 3 are considered in the simulations. A rectangular simply

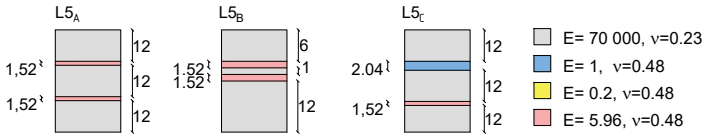

Figure 3: Illustration of the layups used in the analyses with thicknesses (mm), Young modulus E (MPa) and Poisson coefficient of the layers.

supported plate made of 5 alternating layers (layup $L5$) is considered with a transverse distributed load $q = 10^{-3}$ MPa. Geometry, loads and boundary conditions are depicted in Fig. 4. The equilibrium paths are plotted in Fig. 5. The comparisons of the different models confirms the accuracy of the proposed KLWI model also in case of multiple soft layers, unlike the basic KL model. Also in this case, coarse meshes are sufficient to obtained the solid reference solution. It is possible to observe that KLWZ (single ZZ function) proves to be a convenient alternative (fewer DOFs) to KLWI (independent shear deformations) for alternating layups with uniform soft layers, while it results less accurate for non-uniform soft layers.

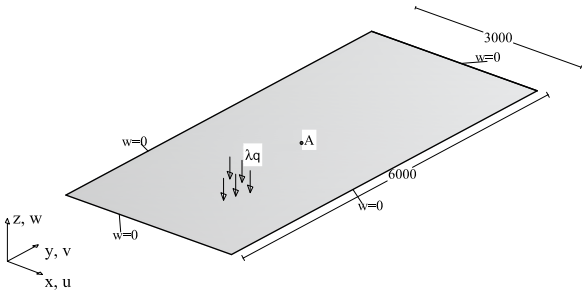

Figure 4: Rectangular plate: geometry (mm), loads, and boundary conditions.

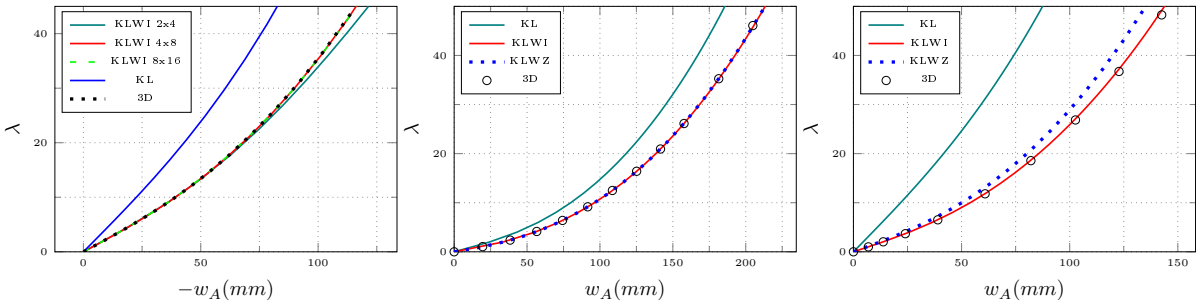

(a) $L5_A$ (b) $L5_B$ (c) $L5_C$

Figure 5: 5-layer rectangular plate: equilibrium paths.

6 CONCLUSIONS

The investigation demonstrated the correctness of the hierarchic formulation in large displacement and buckling problems. Two warping models were studied: 1) independent transverse shear deformations of the soft layers and 2) single zigzag function linking these deformations. The comparison with the reference solid solution showed the great accuracy and reliability of the first warping model, whose number of DOFs depends on the number of soft layers, when usual shell models provide largely wrong predictions. On the other hand, the second warping model allows to reduce the unknowns to five per surface point regardless of the number of layers with no loss of accuracy for uniform soft interlayers. Further details are reported in [18]. The application of the model to thermal loads and temperature-dependent material properties can be found in [19], where the present work is combined with the generalized path-following method developed in [20]. A reduced model cane also obtained for buckling problems as in [21, 22]. Finally, it is wroth citing also [23], where a different model is proposed to include the independent interlayer thickness strain when it is relevant.

REFERENCES

[1] L. Galuppi, G. Royer-Carfagni, Shear coupling effects of the core in curved sandwich beams, Composites Part B: Engineering 76 (2015) 320–331. doi:https://doi.org/10.1016/j.compositesb.2015.01.045.

[2] H. S. Norville, K. W. King, J. L. Swofford, Behavior and strength of laminated glass, Journal

of Engineering Mechanics 124 (1) (1998) 46 – 53. doi:10.1061/(ASCE)0733-9399(1998)124:1(46).

[3] Y. Liang, B. Izzuddin, Nonlinear analysis of laminated shells with alternating stiff/soft lay-up, Composite Structures 133 (2015) 1220–1236. doi:https://doi.org/10.1016/j.compstruct.2015.08.043.

[4] I. V. Ivanov, D. S. Velchev, N. G. Georgiev, I. D. Ivanov, T. Sadowski, A plate finite element for modelling of triplex laminated glass and comparison with other computational models, Meccanica 51 (2016) 341–358. doi:https://doi.org/10.1007/s11012-015-0275-0.

[5] C. Felippa, B. Haugen, A unified formulation of small-strain corotational finite elements: I. theory, Computer Methods in Applied Mechanics and Engineering 194 (21) (2005) 2285–2335. doi:https://doi.org/10.1016/j.cma.2004.07.035.

[6] Y. Liang, F. Lancaster, B. Izzuddin, Effective modelling of structural glass with laminated shell elements, Composite Structures 156 (2016) 47–62, 70th Anniversary of Professor J. N. Reddy. doi:https://doi.org/10.1016/j.compstruct.2016.02.077.

[7] F. G. Flores, Implementation of the refined zigzag theory in shell elements with large displacements and rotations, Composite Structures 118 (2014) 560–570. doi:https://doi.org/10.1016/j.compstruct.2014.07.034.

[8] M. Gherlone, A. Tessler, M. D. Sciuva, C0 beam elements based on the refined zigzag theory for multilayered composite and sandwich laminates, Composite Structures 93 (11) (2011) 2882–2894. doi:https://doi.org/10.1016/j.compstruct.2011.05.015.

[9] J. Simo, D. Fox, On a stress resultant geometrically exact shell model. part i: Formulation and optimal parametrization, Computer Methods in Applied Mechanics and Engineering 72 (3) (1989) 267–304. doi:https://doi.org/10.1016/0045-7825(89)90002-9.

[10] B. Oesterle, R. Sachse, E. Ramm, M. Bischoff, Hierarchic isogeometric large rotation shell elements including linearized transverse shear parametrization, Computer Methods in Applied Mechanics and Engineering 321 (2017) 383–405.

[11] A. J. Herrema, E. L. Johnson, D. Proserpio, M. C. Wu, J. Kiendl, M.-C. Hsu, Penalty coupling of non-matching isogeometric Kirchhoff-Love shell patches with application to composite wind turbine blades, Computer Methods in Applied Mechanics and Engineering 346 (2019) 810–840. doi:https://doi.org/10.1016/j.cma.2018.08.038.

[12] L. Leonetti, D. Magisano, A. Madeo, G. Garcea, J. Kiendl, A. Reali, A simplified Kirchhoff-Love large deformation model for elastic shells and its effective isogeometric formulation, Computer Methods in Applied Mechanics and Engineering 354 (2019) 369 – 396. doi:https://doi.org/10.1016/j.cma.2019.05.025.

[13] A. Tessler, M. D. Sciuva, M. Gherlone, A refined zigzag beam theory for composite and sandwich beams, Journal of Composite Materials 43 (9) (2009) 1051–1081. doi:10.1177/0021998308097730.

[14] T. Hughes, J. Cottrell, Y. Bazilevs, Isogeometric analysis: CAD, finite elements, NURBS, exact geometry and mesh refinement, Computer Methods in Applied Mechanics and Engineering 194 (39) (2005) 4135–4195. doi:https://doi.org/10.1016/j.cma.2004.10.008.

[15] C. Adam, T. Hughes, S. Bouabdallah, M. Zarroug, H. Maitournam, Selective and reduced numerical integrations for NURBS-based isogeometric analysis, Computer Methods in Applied Mechanics and Engineering 284 (2015) 732–761. doi:10.1016/j.cma.2014.11.001.

[16] D. Magisano, L. Leonetti, G. Garcea, How to improve efficiency and robustness of the Newton method in geometrically non-linear structural problem discretized via displacement-based finite elements, Computer Methods in Applied Mechanics and Engineering 313 (2017) 986 – 1005. doi:http://dx.doi.org/10.1016/j.cma.2016.10.023.

[17] D. Magisano, A. Corrado, New robust and efficient global iterations for large deformation finite element analysis of beams and shells with material nonlinearity, Computer Methods in Applied Mechanics and Engineering 406 (2023) 115900. doi:https://doi.org/10.1016/j.cma.2023.115900.

[18] D. Magisano, A. Corrado, L. Leonetti, J. Kiendl, G. Garcea, Large deformation kirchhoff-love shell hierarchically enriched with warping: Isogeometric formulation and modeling of alternating stiff/soft layups, Computer Methods in Applied Mechanics and Engineering 418 (2024) 116556. doi:https://doi.org/10.1016/j.cma.2023.116556.

[19] A. Corrado, D. Magisano, L. Leonetti, G. Garcea, Sensitivity to intensity and distribution of the temperature field in the nonlinear thermo-mechanical analysis of laminated glass plates, International Journal of Non-Linear Mechanics 165 (2024) 104792. doi:https://doi.org/10.1016/j.ijnonlinmec.2024.104792.

[20] F. S. Liguori, D. Magisano, L. Leonetti, G. Garcea, Nonlinear thermoelastic analysis of shell structures: solid-shell modelling and high-performing continuation method, Composite Structures 266 (2021) 113734. doi:https://doi.org/10.1016/j.compstruct.2021.113734.

[21] F. S. Liguori, A. Madeo, D. Magisano, L. Leonetti, G. Garcea, Post-buckling optimisation strategy of imperfection sensitive composite shells using Koiter method and Monte Carlo simulation, Composite Structures 192 (2018) 654–670. doi:https://doi.org/10.1016/j.compstruct.2018.03.023.

[22] F. S. Liguori, D. Magisano, A. Madeo, L. Leonetti, G. Garcea, A koiter reduction technique for the nonlinear thermoelastic analysis of shell structures prone to buckling, International Journal for Numerical Methods in Engineering 123 (2) (2022) 547–576. doi:https://doi.org/10.1002/nme.6868.

[23] L. Leonetti, D. Magisano, G. Garcea, Large rotation isogeometric shell model for alternating stiff/soft curved laminates including warping and interlayer thickness change, Computer Methods in Applied Mechanics and Engineering 424 (2024) 116908. doi:https://doi.org/10.1016/j.cma.2024.116908.